



Accepted Article

Title: Full Meta-substituted 4,4'-Biphenyldicarboxylate Based MOFs:
Synthesis, Structures and Catalytic activities

Authors: Jiawei Li, Yanwei Ren, Chaorong Qi, and Huanfeng Jiang

This manuscript has been accepted after peer review and appears as an Accepted Article online prior to editing, proofing, and formal publication of the final Version of Record (VoR). This work is currently citable by using the Digital Object Identifier (DOI) given below. The VoR will be published online in Early View as soon as possible and may be different to this Accepted Article as a result of editing. Readers should obtain the VoR from the journal website shown below when it is published to ensure accuracy of information. The authors are responsible for the content of this Accepted Article.

To be cited as: *Eur. J. Inorg. Chem.* 10.1002/ejic.201601242

Link to VoR: <http://dx.doi.org/10.1002/ejic.201601242>

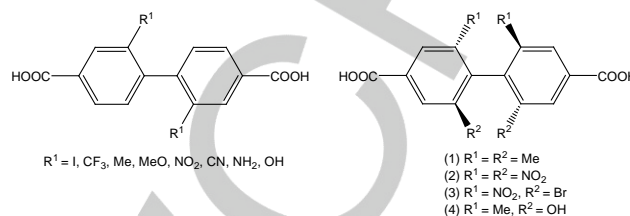
Full *Meta*-substituted 4,4'-Biphenyldicarboxylate Based MOFs: Synthesis, Structures and Catalytic activities

Jiawei Li,^[a] Yanwei Ren,^{*[a]} Chaorong Qi^[a] and Huanfeng Jiang^{*[a]}

Abstract: A full *meta*-substituted 2,2',6,6'-tetramethoxy-4,4'-biphenyldicarboxylic acid (H₂L) has been synthesized and applied in the construction of three metal-organic frameworks (MOFs), ([Cu₃L₃(H₂O)₂(DMF)]_n (**1**), [Zn₄OL₃]_n (**2**) and [Zn₄OL₃(H₂O)(DEF)]_n (**3**). For **1**, the approximately vertical twist of two benzene rings in L leads to the formation of the two-fold interpenetrated 3D structure with 1D open channels (11 Å × 15 Å). **2** and **3** possess the classic two-fold interpenetrated IRMOF structures, and a reversible oxozinc carboxylate clusters transformation between **2** and **3** could be realized *via* solvent-exchanged induced single-crystal-to-single-crystal pathway, which provides a direct structural evidence for Zn₄O core in MOFs as Lewis acidity site. Desolvated framework **1'** exhibits high permanent porosity (Langmuir surface area = 555 m²/g), high thermal stability (up to 300 °C), and highly active properties for cyanosilylation reaction and olefin epoxidation reaction. **2** exhibits moderate carbon dioxide uptake ability and can efficiently catalyze the cycloaddition of CO₂ with epoxides under mild conditions.

Introduction

Metal-organic frameworks (MOFs), emerging as highly designable materials for various applications such as gas adsorption,^[1] photoluminescence,^[2] magnetic,^[3] sensing^[2a, 4] and heterogeneous catalysis,^[5] have been vastly investigated in recent years. The flexible tunability in inorganic metal sites and organic ligands endows MOFs with diverse topology structures and wide practical applications. Especially, judicious selection of ligands plays vital role in determining the underlying topologies, thermal stability, and the consequent properties. Furthermore, MOFs also tend to take the highly ordered crystal structures that can be easily characterized by single crystal X-ray crystallography, which is conducive to their structure-property relations elucidation and function adjustments. The combination of organic ligands and crystal engineering in MOFs synthesis provides a unique platform for rational design and development of MOF-based functional materials.



Scheme 1. Double and full *meta*-substituted BPDC ligands.

Up to now, based on the strong coordination ability, a large number of carboxylate ligands have been used for the construction of MOFs. Among them, the linear rigid aromatic dicarboxylic acid analogues such as 1,4-benzenedicarboxylic acid (BDC),^[6] 4,4'-biphenyldicarboxylic acid (BPDC)^[7] and 1,4-di(4-carboxyphenyl)benzene (TPDC)^[8] have received substantial attention due to their considerable diversities in sizes and functionalities. Recently, reports about the construction of two-substituted BPDC based MOFs are flourishing,^[9] and various functional groups have been introduced into the biphenyl skeleton of BPDC either on the *ortho*- or *meta*-position to the carboxylate groups (Scheme 1). In general, *ortho*-substituted groups may participate in coordination or arouse the change of environment around the metal centers, thus giving rise to some metal-related properties.^[9a-9h] For example, Zhu *et al* have constructed a *ortho*-substituted 3,3'-dimethoxy-4,4'-biphenyldicarboxylic acid for the construction of three novel MOFs^[9g] and found that the attachment of two methoxy groups on the BPDC indeed provide additional coordinating sites to the metals. Alternatively, *meta*-substituted groups of BPDC are not involved in coordination and do not affect the form of classical secondary building units (SBUs) in MOFs. Instead, they make the two benzoate moieties twist mutually, thus rendering an organic building block that is geometrically different from the mother ligand and hence may result in new topologies.^[9i-9z] However, perhaps due to the difficulties in ligands synthesis, less attention^[10] are paid to the full *meta*-substituted BPDC ligands (Scheme 1) although they can probably make MOFs high thermal stabilities, rich topology structures, potential axial chirality, and reduction of framework interpenetrations based on the space-filling effect and implanarity of biphenyl units. For examples, Christoph *et al* synthesized a BPDC analog (H₂Me₄BPDC) with full *meta*-substitution by methyl groups, and found that the corresponding MOFs ([Zn₄O(Me₄BPDC)]₃) and [Cu₂(Me₄BPDC)₂] exhibit better adsorptive properties towards H₂ and CO₂ than those of nonmethylate parent ligand based MOFs, owing to more increasing lipophilicity of Me₄BPDC than that of BPDC.^[10a] Therefore, the synthesis and application of new MOFs by using multisubstituted aromatic dicarboxylic acids are highly desirable.

On the other hand, Lewis acid catalysis is of vital importance in organic transformations. Although many homogeneous Lewis acid catalysts, such as ZnCl₂ and Cu(NO₃)₂, usually exhibit high

[a] Key Laboratory of Functional Molecular Engineering of Guangdong Province, School of Chemistry and Chemical Engineering, South China University of Technology, Guangzhou 510640, P. R. China. E-mail: renyw@scut.edu.cn, jianghf@scut.edu.cn http://www.scut.edu.cn/ce/

Supporting information for this article is given via a link at the end of the document

activity and selectivity, their practical applications remain limited because of the difficulty in catalyst/product separation. The immobilization of homogeneous catalysts can facilitate their recovery and reuse and therefore is of considerable interest to academia and industry. MOFs often possess high catalytic sites loading, open channels and high thermal stability, providing an effective platform for the rational design of efficient heterogeneous catalysts.

In this contribution, a new full *meta*-substituted BPDC ligands 2,2',6,6'-tetramethoxy-4,4'-biphenyldicarboxylic acid (H_2L) and corresponding MOFs ($[Cu_3L_3(H_2O)_2(DMF)]_n$ (**1**), $[Zn_4OL_3]$ (**2**), and $[Zn_4OL_3(H_2O)(DEF)]_n$ (**3**)) were synthesized and characterized by single crystal X-ray diffraction, powder X-ray diffraction (PXRD), thermogravimetric analyses (TGA) and infrared spectroscopy (IR). A reversible oxozinc carboxylate clusters transformation between **2** and **3** *via* solvent-exchanged induced single-crystal-to-single-crystal (SCSC) process is reported, which provides a direct structural evidence for Zn_4O core in MOFs as Lewis acidity site. Furthermore, we investigated the catalytic properties of desolvated framework **1** and **2**, respectively. **1** turned out to be an efficient heterogeneous catalyst for epoxidation reaction and cyanosilylation reaction. **2** displayed excellent catalytic properties for the synthesis of cyclic carbonates from epoxides and CO_2 under mild conditions.

Results and Discussion

Crystal Structures

1 crystallizes in the monoclinic space group $P2_1/n$. There are three Cu^{2+} ions, three L ligands, one DMF molecule and two H_2O molecules in the asymmetric unit (Figure S1, in Supporting Information, SI). The SBUs of **1** are the classic paddle-wheel $[Cu_2(O_2CR)_4]$ units in which four carboxyl groups from four ligands bridge two Cu^{2+} in bidentate fashion (Figure 1a). The Cu-O (1.939–2.142 Å) and Cu-Cu (2.6340–2.6390 Å) distances in **1** are comparable to those in previously reported $[Cu_2(O_2CR)_4]$ based MOFs.^[9g, 9z, 10a, 11] Note that two types of SBU structures with varied axially coordinated solvent molecules are formed in the self-assembly synthetic process. As is shown in Fig.1b, the two Cu atoms of SBU-1 are axially coordinated by two H_2O molecules while the adjacent SBU-2 is linked by one water molecule and one DMF molecule. A twist of 80.98° between two benzene rings in L ligand leads to the verticality of adjacent SBU, which facilitates the extension of linkers to other two orientations and predetermines the formation of the final 3D framework. It has to be pointed out that unsubstituted rigid dicarboxylic acid BPDC always result in a 2D layer structure, as the benzene rings of BPDC stay in the same plane, thus rendering coplaner 4-connected nodes through the networks. Attempts to build 3D frameworks by BPDC usually need auxiliary ligands to work as pillars, which regrettably limits axial degree of freedom at the same time. Here in this case, the full *meta*-substituted ligand with benzene rings moving out of the same plane, constructs *nbo* type 3D framework without pillar linkers (Figure 1c and 1d). Consequently, the axial positions are available for solvent

molecules that can be removed to expose the Cu^{2+} active sites for catalytic reactions. To our knowledge, reports of the presented *nbo* type Cu-MOF built from only one rigid dicarboxylic acid ligand are relatively limited.^[9k, 9z, 10a, 12] The voids of the framework, although blocked by OCH_3 groups to some extent, are still large enough to allow for double interpenetration (Figure 1e), and notable 1D channels size up to $11\text{Å} \times 15\text{Å}$ (atom-to-atom distance) can be found along *a* axis. The solvent accessible voids calculated using PLATON is as high as 62.07% (7770 Å^3 out of 12517 Å^3). Although precise solvent content cannot be determined by X-ray crystallography resulting from their disordered nature, by means of the SQUEEZE routine of PLATON, EA and TG it is found that the void space is filled by the DMF and water molecules.

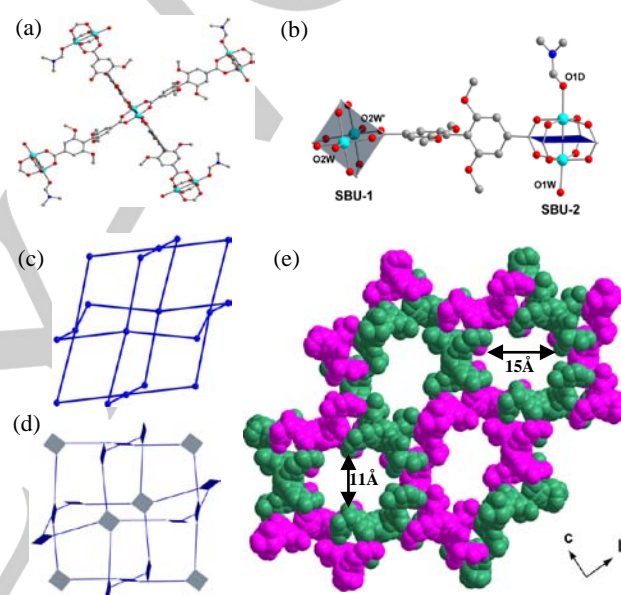


Figure 1. (a) $[Cu_2(O_2CR)_4]$ paddle-wheel structure in **1**. (b) two kinds of $[Cu_2(O_2CR)_4]$ paddle-wheel units linked by L to illustrate the twist of square-planar SBUs. (c) *nbo* net and (d) augmented *nbo* net where the point vertices of the net are replaced by the different square paddle-wheel vertex figures. (e) double interpenetrations of **1** along *a* axis.

2 crystallizes in the trigonal $R\bar{3}$ space group. There are two Zn^{2+} ions, one L ligand and one μ_4-O atom in the asymmetric unit (Fig. S2). The SBU of **2** is based on the classic IRMOF series $[Zn_4O(O_2CR)_6]$ where six carboxyl groups from six ligands bridge four Zn^{2+} in bidentate fashion. Each Zn atom connects three O atoms from three L ligands and one μ_4-O atom, displaying tetrahedral coordination geometry. **2** adopts a two-fold interpenetrated structure with 54.6% of void space as calculated by PLATON that is filled by DMF and water molecules. The largest dimensions of open channels are $6\text{Å} \times 4\text{Å}$ (atom-to-atom distance). From topological perspective, the Zn_4O core can be viewed as 6-connected nodes which are further connected by ligands, simplified as rods, to construct the final 3D network with *pcu* topology.^[13] It is noteworthy that, when the crystals of **2** were immersed in DEF solution for 72 h at room temperature, we successfully obtained new colorless block crystals with the formula of $[Zn_4OL_3(H_2O)(DEF)]$ (**3**) that crystallized in the triclinic

P-1 space group confirmed by single crystal X-ray diffraction analysis. The most prominent structural distinction differing from **2** is that one of the Zn atoms in the Zn₄O core of **3** is further coordinated by one DEF molecule and one water molecule, adopting octahedral coordination geometry instead (Figure 2). The Zn-O (μ_4 -O) bonds lengths in **3** are very similar to those in **2**, while the Zn-O_{carboxylate} bonds around Zn are slightly longer (with the average elongation of *ca.* 0.15 Å) than the corresponding distances in **2** due to the coordination of H₂O and DEF molecules. **3** still represents a two-interpenetrated framework with larger cavities inside network than those in **2** due to a slight spatial displacement of ligands. A literature survey shows that there are only a few structurally characterized [Zn₄O(O₂CR)₆] based MOFs with coordinated water molecules, and they were all prepared by direct synthetic methods.^[14]

More interestingly, when crystals of **3** were immersed in the weaker donor solvent THF for 96 h at room temperature, it can transition back to the trigonal framework (*R*-3 space group) with a formula of [Zn₄OL₃]:2THF (**2'**) that is determined by single crystal X-ray diffraction analysis. Although several examples of SCSC transformations were reported for MOFs,^[15] this is the first example where [Zn₄O(O₂CR)₆] based MOFs exhibit a reversible SCSC structural transformation induced by solvent exchange. Our observations can be valuable in the discussion about the catalytic activity of [Zn₄O(O₂CR)₆] based MOFs, as well as in the construction of reliable frameworks models for computational studies on these MOFs. Very recently, utilizing first-principles molecular dynamics simulations, multinuclear solid-state nuclear magnetic resonance and mass spectrometry, Dincă M reported that the zinc centers in MOF-5 could bind solvent molecules (such as DMF), thereby increasing their coordination number and dynamically dissociate from framework itself.^[16]

Thermogravimetric analysis and powder X-ray diffraction analyses

TGA were performed to investigate the stability of the MOFs **1-3** (Figure 3). The TGA curve of **1** shows a weight loss of ~15% from 30 °C to 320 °C, corresponding to the loss of disordered water molecules, DMF molecules and coordinated water molecules, DMF molecules in the channels. The intense weight loss from 320 °C indicates the collapse of the framework. Based on above result, we then performed the PXRD measurement of the as-synthesized sample **1** and desolvated sample **1'** that obtained by heating **1** at 200 °C in vacuum pressure to remove coordinated and non-coordinated solvent molecules. As shown in Figure 4, the comparison of as-synthesized and simulated PXRD form crystal structure confirms the phase purity of the bulk sample, and the result of desolvated sample also match very well with simulate date, indicating no obvious structural change, which demonstrates that **1** possesses stable microporosity.

TGA curve of **2** shows a weight loss of ~25.0% from room temperature to 350 °C, corresponding to the loss of disordered water molecules and DMF molecules. The SCSC product **3** exhibits similar TGA curve and almost the same weight loss with **2**. The phase purity of bulky sample of **2** were confirmed by PXRD analysis in which the patterns of the as-synthesized

samples are in excellent agreement with the simulated ones (Figure 5).

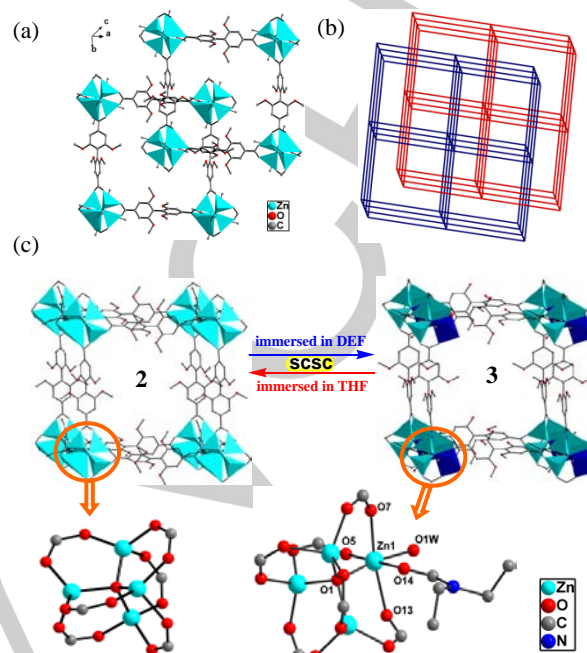


Figure 2. (a) double interpenetrations of **2**. (b) *pcu* network of **2**. (c) reversible oxozinc carboxylate clusters transformation of **2** and **3** via SCSC process and structures of Zn₄O cores in **4** and **5**. Blue polyhedron in **5** represents the six-coordinated zinc center.

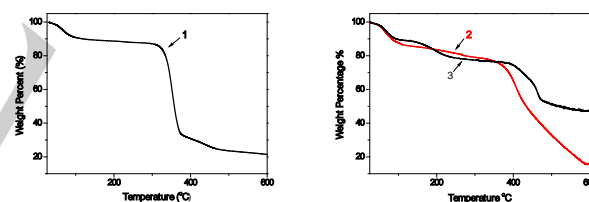


Figure 3. Thermogravimetric analyses of **1-3**.

Gas sorption

For the gas sorption measurement, we firstly immersed the samples of **1** and **2** in MeOH for 2 days to exchange the high-boiling DMF with MeOH molecules. The samples were subjected to activate at 100 °C in vacuum for 12 h and then were ready for the sorption test. We have determined the permanent porosity of **1'** by nitrogen adsorption at 77 K. The N₂ adsorption isotherm of **1'** reveals Type I behavior, indicative of microporous materials (Figure 6). From these data, the apparent surface area was calculated using the Langmuir method to be 555 m²/g (412 m²/g BET), thus confirming the permanent porosity of **1'**. The CO₂ adsorption property of **1** and **2** were also investigated (Figure 7). The results show that CO₂ uptake of **1** (~29.0 cm³/g) is higher than that of **2** (~13.0 cm³/g) at 273 K at 1.0 atm, indicating the unsaturated metal site [Cu₂(O₂C)₄] unit in **1'** has high affinity for CO₂ molecules, which is agreement with the results observed in previous literatures.^[11,17]

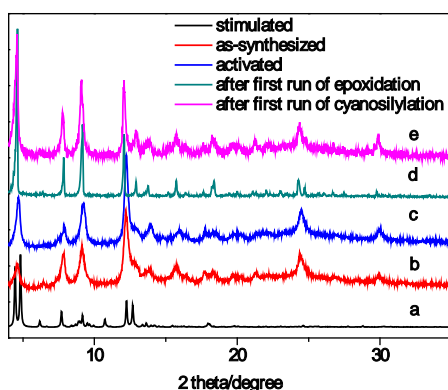


Figure 4. PXRD patterns of **1**: (a) **1** simulated from CIF file, (b) as-synthesized sample of **1**, (c) activated sample **1'**, (d) recovered **1'** after first run of epoxidation, (e) recovered **1'** after first run of cyanosilylation.

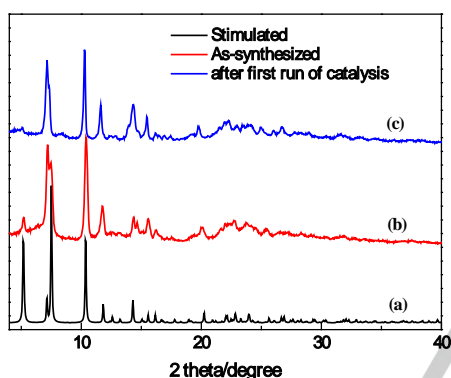


Figure 5. PXRD patterns of **2**: (a) **2** simulated from CIF file, (b) as-synthesized sample of **2**, and (c) recovered **2** after first run of catalysis.

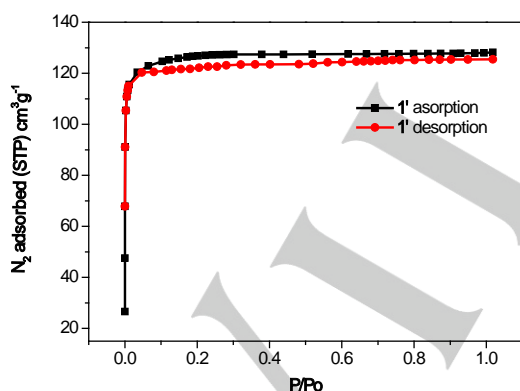


Figure 6. N₂ adsorption isotherm of **1** at 77K.

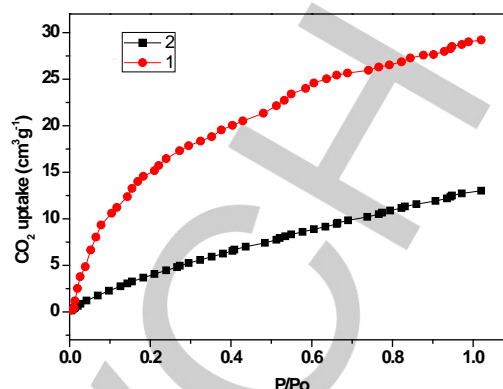


Figure 7. CO₂ adsorption isotherms of **1** and **2** at 273K.

Catalytic Performances

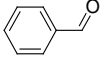
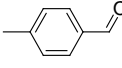
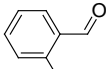
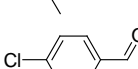
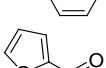
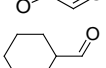
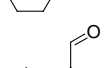
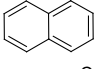
Cyanosilylation Reaction

Cyanosilylation of carbonyl compounds is one of the most important Lewis acid catalyzed reaction as it provides key derivatives in the synthesis of fine chemicals. Thus, we conducted cyanosilylation to examine the Lewis acid activity of the desolvated **1'**. When benzaldehyde was taken as the standard substrate, **1'** presents high conversion and selectivity (99%) at 313 K for 4 h, while the control reaction shows only a little conversion (8%) under the same conditions without the catalyst. This catalytic activity is comparable to other Cu-based MOFs^[18] in the cyanosilylation of benzaldehyde. The scope of the reaction was further explored with various aldehydes using **1'** as catalyst, and the results are summarized in Table 1. The aromatic aldehydes with electron-withdrawing or electron-donating groups both gave excellent conversions and selectivity (Table 1, entries 2-4). Heterocyclic furan aldehyde also participated well in this reaction with quantitative conversions (Table 1, entry 5). Moreover, aliphatic cyclic aldehyde still did not show any significant decrease of the conversion and selectivity (Table 1, entry 6). However, with the size extension of the substrates, the conversion drops dramatically. For example, the conversions of 1-naphthaldehyde and 9-anthraldehyde are 50% and 7%, respectively (Table 1, entries 7 and 8). A significant degradation of the conversion suggests that large substrates are more difficult to enter into catalyst's channels, relative to small ones. Obviously, these catalytic reactions mainly occur in the channels of **1'**. The smaller the substrate size the faster the rate of entering into the channel and then the higher the catalytic activity. Additionally, acetophenone exhibited much weaker reactivity, partly because of the lower inherent reactivity of ketones, as found in most cases.^[19]

Recyclability of **1'** was studied for this reaction. After the processes of centrifugation, washing and drying, the recovered catalyst was reused five times without significant loss of reactivity (Figure 8). Moreover, the catalyst recovered from the first run cyanosilylation exhibited almost the same PXRD pattern as the fresh **1'** (Figure 4), unambiguously supporting the stability

of framework during the catalytic reaction. Atomic absorption spectrophotometry (AAS) analysis of the filtrate indicated that the concentration of Cu^{2+} is only 8.84 ppm, indicating that the leaching of Cu^{2+} into the solvent was negligible during the reaction. These results and hot filtrate experiments data (Figure S6) confirm the heterogeneous nature of this catalytic reaction.

Table 1. Cyanosilylation reaction of various aldehydes catalyzed by **1'**.^[a]

Entry	Substrates	Conv.(Select.) ^[b] [%]
1		99 (99)
2		99 (99)
3		99 (99)
4		99 (99)
5		99 (99)
6		99 (99)
7		50 (99)
8		7 (99)

[a] Reaction condition: **1'** (3.5 mg, 0.5 mol%), substrate (0.5 mmol), TMSCN (1 mmol) were stirred without solvent at 40 °C for 4 h under N_2 atmosphere. [b] conversion and selectivity were determined by GC-MS with dodecane as internal standard.

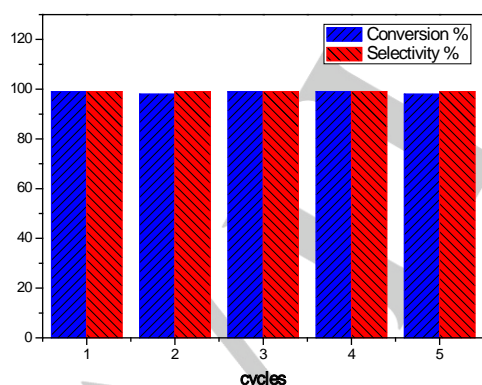


Figure 8. Recyclability test of **1'** for the cyanosilylation reaction.

Olefin Epoxidation Reaction

With the above good results in hand, we then evaluated the catalytic activities of **1'** toward epoxidation of olefins, since olefin epoxidation is a highly important oxidation reaction catalyzed by

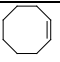
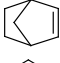
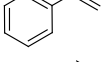
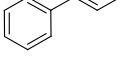
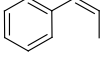
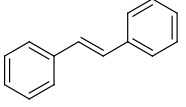
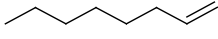
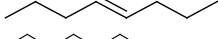
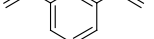
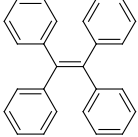
various metal salts under homogeneous or heterogeneous conditions.^[20] However, reports of olefin epoxidation reactions related to heterogeneous catalytic studies on Cu-based MOFs have been extremely scarce.^[5f, 21] We have reported a 2D Cu-based MOFs constructed by a tritopic carboxylate ligand, tris(4'-carboxybiphenyl)amine, demonstrating an excellent activity and selectivity for olefin epoxidation reactions using *t*-BuOOH as an oxidant for the first time.^[5f] Recently, Wang reported a nanoscaled MOF $[\text{Cu}_3(\text{BTC})_2]_n$ presents efficient activity in aerobic epoxidation reaction with molecular oxygen as an oxidant and trimethylacetaldehyde as a sacrificial co-reductant.^[21d]

Initially, we chose cyclooctene as the model substrate to identify the optimal reaction conditions. The optimized reaction conditions involved olefin (0.5 mmol), trimethylacetaldehyde (1 mmol), catalyst **1'** (1 mmol%) at 40 °C for 6 h under 1 atm. O_2 . It is mentioned that trimethylacetaldehyde as a sacrificial co-reductant in this reaction, is crucial to improve the conversions and selectivity (Table S1).^[21d] Compared with other reports in which *t*-BuOOH served as an oxidant, our catalytic system has higher conversion and selectivity.^[21] In the case of the applicability of the substrates, oxidation of nonterminal olefins such as norbornene, *trans*- β -methylstyrene, *cis*- β -methylstyrene and *trans*-stilbene, occurs with high 99% conversion and 99% selectivity (Table 2, entries 2 and 4-6). For terminal styrene, **1'** exhibits better conversion and selectivity than that of nanoscaled $[\text{Cu}_3(\text{BTC})_2]_n$ under same reaction conditions,^[21d] despite the dominant reaction involved the formation of styrene oxide and benzaldehyde (Table 2, entry 3). In addition, linear aliphatic alkenes are generally considered as inert olefins towards epoxidation. To our surprise, 1-octene and *trans*-4-octene were also oxidized in moderate conversions and with excellent selectivities, and similarly, internal olefin exhibits higher activity than the terminal olefin (Table 2, entries 7 and 8). Under optimized conditions, the oxidation of 1,3-diethylbenzene was also tested (Table 2, entry 9), and the results showed that the ratio of double oxidized product versus the mono oxidized product was 58:3, which indicates the substrate tended to be completely oxidized. We attribute this relatively high selectivity to the high density and suitable position of catalytic sites in channels of **1'**. To date, the preparation of divinylbenzene dioxide has been less reported, and most of them only gave poor conversions and selectivity.^[22] Thus, the result found here provides a profound direction to the synthesis of divinylbenzene dioxide. Bulky size substrate, 1,1,2,2-tetraphenylethene which was much larger than the available pore dimensions of **1'**, gave no any conversion under optimized conditions, revealing that the substrate was too large to diffuse through the channels of **1'**. On the contrary, the homogeneous catalyst $\text{Cu}(\text{NO}_3)_2$ could promote this reaction with 40% conversion. This comparison suggests that the heterogeneous catalysis reaction took place in the channels, not on the surface of the framework, as similar as in cyanosilylation reaction. AAS analysis indicated almost no leaching of Cu (6.14 ppm) during the catalytic process.

Also, **1'** can be recovered by centrifugation, washing with methanol, and then drying. Recyclability experiment showed that the reaction proceed well in five successive runs without

apparent loss of catalytic efficiency (Figure 9). The match of PXRD patterns of the recovered **1'** and fresh sample confirms the stability of framework during the catalytic reaction (Figure 4).

Table 2. Aerobic olefin epoxidations catalyzed by **1'**.^[a]

Entry	Substrates	Conv.(Select.) ^[b] [%]
1		99 (99)
2		99 (99)
3		90 (88)
4		99 (99)
5		99 (99)
6		99 (99)
7		46 (93)
8		80 (88)
9		99 (58:3 ^[c])
10		<1

[a] Reaction conditions: **1'** (7 mg, 1 mol%), substrate (0.5 mmol), trimethylacetaldehyde (1 mmol) were stirred in 2.5 mL of CH₃CN at 40 °C for 6 h with 1 atm. O₂. [b] conversion and selectivity were determined by GC-MS with dodecane as internal standard. [c] the ratio of double oxidized product versus the mono oxidized product.

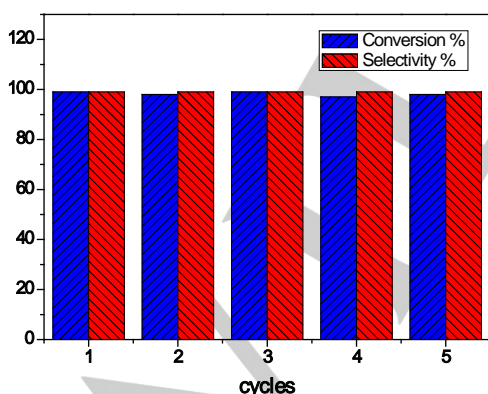


Figure 9. Recyclability test of **1'** for olefin epoxidation reaction.

Cycloaddition reaction of CO₂ with epoxides

Recent literatures have proved that MOFs possessing Lewis acid sites are excellent heterogeneous catalysts for the cycloaddition reaction of CO₂ with epoxides.^[23] The reversible

SCSC process between **2** and **3** in solution prompted us to investigate their catalytic performances for this reaction. As a benchmark substrate, we select 2-(phenoxymethyl)oxirane as epoxide, and the results are summarized in Table S2. After several kinds of reaction variables were investigated, the optimized reaction conditions involved epoxide, 1 atm. of CO₂ in the presence of 0.3 mol % of **2** and 2.5 mol % of *n*Bu₄NBr at 50 °C, with 86% conversion and 99% selection for cyclic carbonate. The activity of **2**/*n*Bu₄NBr was similar to that of heterogeneous MOF-5/*n*Bu₄NBr system^[23a] and homogeneous ZnCl₂/*n*Bu₄NBr system.^[24] However, under the optimized conditions, **1'** was capable of catalyzing this reaction with a relative low conversion (Table S2). This is in accordance with that Zn²⁺ ion usually shows increased Lewis-acid behavior as a result of the constrained geometry imposed by ligands.^[25] Next, **2**/*n*Bu₄NBr system was applied for various epoxides, such as epichlorohydrin, 2-vinylloxirane, styrene oxide, 2-butyloxirane and cyclohexene oxide (Table 3). The very good conversions of epichlorohydrin and 2-vinylloxirane (Table 3, entries 1 and 2) can be explained by the electron-withdrawing substituents. These substituents result in facilitated nucleophilic attack of Br⁻ during the ring opening of the epoxides. The comparatively moderate conversion of styrene oxide might be ascribed to the low reactivity at the β-carbon center (Table 3, entry 3). Cyclohexene oxide gave low conversions, which was attributed to the steric hindrance posed by the cyclohexene ring (Table 3, entry 6).^[26]

After catalytic reaction, AAS analysis of the reaction mixture filtrate revealed negligible Zn²⁺ leaching (5.41 ppm), indicating the catalytic reaction is indeed heterogeneous in nature. Furthermore, the recovered **2** could be used in successive five cycles without significant loss of catalytic efficiency (Figure 10). PXRD pattern of the recovered **2** showed its framework still maintained after the catalytic reaction (Figure 5). Based on above catalytic data and the mutual transformations between tetrahedral and octahedral geometry configuration for one of zinc center of Zn₄O cores through SCSC transformations, we proposed that the coupling reaction is initiated by coordination of the Zn₄O cores in **2** with the oxygen atom of epoxide, accompanying with the coordination configuration changing of one zinc center from tetrahedral to octahedral geometry (Scheme 2). Secondly, the Br⁻ generated from *n*Bu₄NBr attacks the less-hindered carbon atom of the coordinated epoxide to form an alkoxide. Then, this intermediate can react with the activated CO₂ to give the corresponding cyclic carbonates.^[23a] We speculate that in all steps, the Zn-O_{carboxylate} bonds did not break, and thus the integrity of Zn-MOFs framework maintained.

Table 3. Various carbonates synthesis catalyzed by **2**.^[a]

Entry	Epoxides	Conv.(Select.) ^b [%]
1		96 (99)
2		99 (81)
3		55 (99)
4		86 (99)
5		73 (99)
6		13 (5)

[a] Reaction conditions: epoxide (2 mmol), **2** (0.3 mol% Zn₄O core) and *n*Bu₄NBr (2.5 mol%) under CO₂ (1 atm. pressure), reaction time 4h, reaction temperature 50 °C. [b] Conversion and selectivity were determined by GC-MS with dodecane as internal standard.

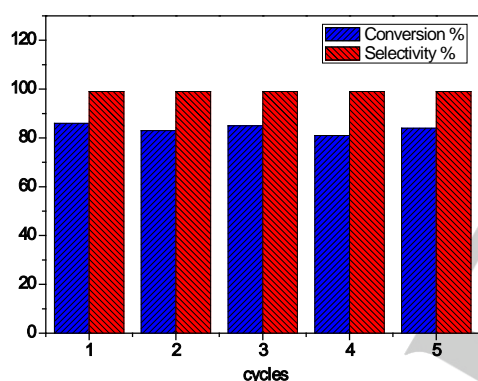
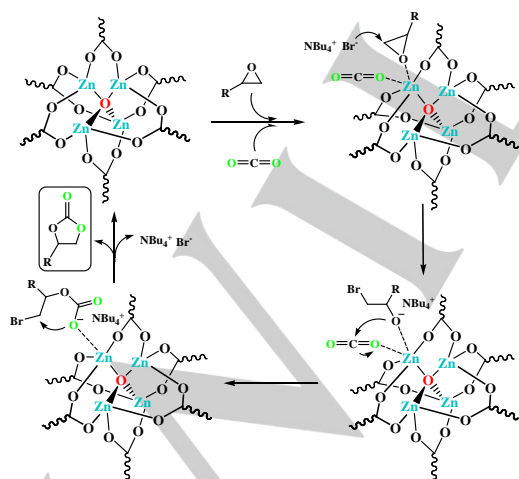


Figure 10. Recyclability test of **2** for the cycloaddition reaction of CO₂ with epoxides.



Scheme 2. Proposed mechanism of the cycloaddition reaction of epoxides and CO₂ catalyzed by **2**/*n*Bu₄NBr.

Conclusions

In summary, we have successfully constructed three new MOFs based on a rigid and full *meta*-substituted 4,4'-biphenyldicarboxylic acid by using solvothermal method. The catalytic results demonstrate that desolvated **1'** can act as a highly efficient, high stable, easily recyclable, and size-selective heterogeneous catalyst for cyanosilylation and olefin epoxidation reactions. In addition, *via* reversible SCSC process, we firstly found the Zn₄O core in **2** can coordinate H₂O and DEF with changing coordination geometry around zinc atom but no breaking of Zn-O_{carboxylate} bonds, and preserving the MOFs framework essentially unchanged. Such finding is quite important for a better understanding of how Zn₄O core in MOFs plays a Lewis acid catalytic role. As an example, **2**/*n*Bu₄NBr system exhibits excellent performance in the preparation of cyclic carbonates from epoxides with CO₂ under mild conditions.

Experimental Section

Materials and Methods

All solvents were purchased from commercial suppliers and used without further purification. Powder X-ray diffraction (PXRD) patterns were collected on a Bruker D8 powder diffractometer at 40kV, 40mA with Cu K α radiation ($\lambda=1.5406\text{\AA}$), with a scan speed of 17.7 s/step and a step size of 0.01995 $^\circ$ (2 θ). Thermogravimetric analyses (TG) were performed on a Q600 SDT instrument under a flow of N₂ at a heating rate of 10 °C/min. NMR were done on a Bruker Model AM-400 (400 MHz) spectrometer. Elemental analyses (EA) for C, H and N were carried out using a Vario EL III Elemental Analyzer. Infrared (IR) spectra were measured from a KBr pellets on a Nicolet Model Nexus 470 FT-IR spectrometer in the range of 4000-400 cm⁻¹. N₂ and CO₂ adsorption experiments were performed with a Quantachrome AS-1 MP. The content of metal ions was determined by Atomic Absorption Spectrometer (Z-2000, HITACHI). Gas chromatography-mass spectrometry (GC-MS) spectrometry was recorded on Shimadzu Model GCMS-QP5050A system that was equipped with a 0.25mm \times 30m DB-WAX capillary column.

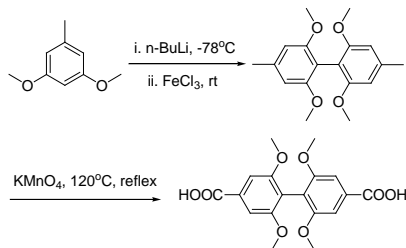
Synthesis of Ligand

H₂L was synthesized by a Fe-catalyzed oxidation coupling of 3,5-dimethyltoluene, followed by KMnO₄ oxidation of the methyl to the carboxyl, as shown in Scheme 3.

I. Synthesis of 2,2',6,6'-tetramethoxy-4,4'-dimethylbiphenyl. To a mixture of 3,5-dimethoxytoluene (3.04 g, 20 mmol) and tetramethylethylenediamine (2.78g, 24mmol) in dry THF (50 mL) was added *n*BuLi (20 mL, 22 mmol, 2.2 M in hexane) at -78 °C. After stirring for 5 min at -78 °C, the temperature was raised to 0 °C. 2.5 h later, FeCl₃ (3.88 g, 24 mmol) was added in portions and then reaction mixture was warmed to room temperature. After stirring for 8 h at room temperature, about 50 mL of HCl (1 M) was added and the mixture was extracted with ethyl acetate (50 mL \times 3). The organic layers were dried over anhydrous Na₂SO₄. After evaporation under reduced pressure, the residue was washed with hexane to give the products (1.9 g, 65% yield). ¹H NMR (CDCl₃): δ = 6.47(s, 4H); 3.70(s, 12H); 2.38(s, 6H). ¹³C NMR (CDCl₃): δ = 158.23, 138.65, 109.57, 105.58, 56.12, 22.33.

II. Synthesis of H₂L. KMnO₄ (15.8 g, 100 mmol) was added in several portions at regular intervals over a period of 5 d to a solution of 2,2',6,6'-tetramethoxy-4,4'-dimethylbiphenyl (3.02 g, 10 mmol) in pyridine/water (v/v, 4:1, 100 mL) at refluxing state. Next, the pyridine and most of the water

were removed in vacuo, and the brown solid was filtered off. The filtrate was acidified (pH = 1) with concentrate HCl and the resulting precipitate was collected by filtration to give the products (2.61 g, 72%). M.p. 343–345 °C; ¹H NMR (DMSO-*d*₆): δ = 12.98(s, 2H); 7.23(s, 4H); 3.68(s, 12H). ¹³C NMR (DMSO-*d*₆): δ = 167.17, 157.59, 131.71, 116.11, 104.97, 55.77. IR data (KBr pellet, *v*/cm⁻¹): 3602, 2934, 1690, 1578, 1461, 1409, 1318, 1262, 1228, 1125, 1000, 864, 772, 725. HR-MS: *m/z*, 385.0892 (M+Na⁺).



Scheme 3. Synthesis of ligand H₂L.

Synthesis of [Cu₃L₃(H₂O)₂(DMF)]_n (**1**)

Solvothermal reaction of Cu(NO₃)₂·3H₂O (6 mg, 0.025 mmol) and H₂L (9 mg, 0.025 mmol) was performed in a solvent mixture of DMF/H₂O (1 mL/0.1 mL) in a 10 mL vial and heated at 70 °C for one day, then the reaction was cooled to room temperature at a rate of 5 °C/h. Deep blue crystals were isolated by decanting the mother liquor and washing with DMF and H₂O. Yield: 25 mg (73%). IR data (KBr pellet, *v*/cm⁻¹): 3593, 3006, 2940, 2840, 1658, 1563, 1458, 1401, 1311, 1222, 1123, 999, 871, 789, 760, 451. Elemental analysis, calcd. for [Cu₃L₃(H₂O)₂(DMF)](DMF)₂(H₂O): C, 48.96; H, 4.86; N, 2.72. Found: C, 48.78; H, 4.70; N, 2.58.

Synthesis of [Zn₄OL₃]_n(**2**)

Solvothermal reaction of Zn(NO₃)₂·6H₂O (8 mg, 0.025 mmol) and H₂L (4.5 mg, 0.0125 mmol) was performed in a solvent mixture of DMF/H₂O (1 mL/0.1 mL) in a 10 mL vial and heated at 90 °C for three days, then the reaction was cooled to room temperature at a rate of 5 °C/h. The product was isolated by decanting the mother liquor and washing with DMF and H₂O. Yield: 10 mg (57%). IR data (KBr pellet, *v*/cm⁻¹): 3606, 2941, 2838, 1558, 1458, 1403, 1223, 1122, 999, 871, 789, 761, 443. Elemental analysis, calcd. for [Zn₄OL₃](DMF)₂(H₂O)₃: C, 46.20; H, 4.36; N, 1.79. Found: C, 46.12; H, 4.30; N, 1.73.

Synthesis of [Zn₄OL₃(H₂O)(DEF)]_n(**3**)

3 was synthesized by single-crystal-to-single-crystal (SCSC) process. About 5 mg of crystals of **2** were immersed in N,N'-diethylformamide (DEF) solution for 72 h at room temperature, producing new colorless block crystals. IR data (KBr pellet, *v*/cm⁻¹): 3603, 2939, 2841, 1559, 1450, 1399, 1221, 1119, 1002, 868, 780, 763, 448. Elemental analysis, calcd. for [Zn₄OL₃(H₂O)(DEF)](DEF)₂(H₂O): C, 48.77; H, 5.01; N, 2.47. Found: C, 48.69; H, 4.95; N, 2.41.

Crystal Structure Determinations

Single crystal X-ray diffraction analyses of MOFs **1–3** were performed on an Xcalibur Onyx Nova four-circle diffractometer using CuKα radiation (λ = 1.54184 Å) at 100 K. The empirical absorption corrections were performed using the CrystalClear program. The structures were solved by direct methods and refined on *F*² by full-matrix least-squares technique using the SHELX-97 program package.^[27] The metal atoms in the asymmetric unit were located first, followed by the other atoms in the main framework from the Fourier difference map. SQUEEZE subroutine of PLATON software suite^[28] was applied to remove the scattering from the highly disordered guest molecules for MOFs **1–3** and then the resulting new HKL file was used to further refine the structure. All non-hydrogen atoms were refined with anisotropic displacement parameters.

Hydrogen atoms were placed in geometrically idealized positions and refined using a riding model. Cambridge Crystallographic Data Centre files CCDC: 1490502 (for **1**), 1448509 (for **2**), and 1448510 (for **3**) contain the supplementary crystallographic data for this paper. Relevant crystallographic data were given in Table 4.

Table 4. Crystallographic data and structure refinement for **1–3**.

MOFs	1	2	3
Empirical formula	C ₅₇ H ₅₉ Cu ₃ N O ₂₇	C ₅₄ H ₄₈ O ₂₅ Zn ₄	C ₅₉ H ₆₁ NO ₂₇ Zn ₄
Formula weight	1380.67	1558.68	1697.87
T (K)	100(2)	100(2)	100(2)
Wavelength (Å)	1.54178	1.54178	1.54178
Crystal system	Monoclinic	Trigonal	Triclinic
Space group	<i>P</i> 2 ₁ / <i>n</i>	<i>R</i> -3	<i>P</i> -1
<i>a</i> / Å	15.3035(3)	24.763(5)	16.828(9)
<i>b</i> / Å	39.6946(6)	24.763(5)	16.962(5)
<i>c</i> / Å	21.5934(5)	28.146(9)	17.034(1)
α°	90	90°	94.81°
β°	107.402(2)	90°	95.54°
γ°	90	120°	91.60°
<i>V</i> / Å ³	12516.9(4)	14947.82	4819.52
<i>Z</i>	4	6	2
ρ / g·cm ⁻³	0.733	0.905	1.018
μ / mm ⁻¹	0.957	1.511	1.614
<i>F</i> (000)	2844	4152	1516
θ range data collection	2.23–71.73	2.59–71.63	2.62–66.08
Reflections collected	56706	11881	16342
Unique	23995	6277	16342
Data/restraints/parameters	23995/0/793	6277/0/266	16342/5/800
GOF on <i>F</i> ²	0.922	1.103	0.943
<i>R</i> ₁ , <i>wR</i> ₂ [<i>></i> 2σ(<i>I</i>)]	0.0557, 0.1400	0.0798, 0.2338	0.0620, 0.1543
<i>R</i> ₁ , <i>wR</i> ₂ (all data)	0.0762, 0.1491	0.0959, 0.2527	0.0850, 0.1663

Catalytic Experiments

Cyanosilylation reaction. The cyanosilylation reaction was carried out in a sealed tube with magnetic bar. **1** was activated at 200 °C for 5 h under vacuum pressure to remove the coordinated water molecules before use. A mixture of carbonyl compounds (0.5 mmol), trimethylsilyl cyanide (TMSCN) (99 mg, 1 mmol), and **1'** (3.5 mg, 0.5 mol%) were stirred at 40 °C for 4 h under N₂ atmosphere. After completion, the mixture was filtered to remove the solid phase and the filtrate was analyzed with GC-MS (using dodecane as the internal standard).

Olefin Epoxidation Reaction. The epoxidation reaction was carried out in a glass tube with magnetic bar. **1** was activated at 200 °C for 5 h under vacuum pressure to remove the coordinated water molecules before use. A mixture of olefin (0.5 mmol), **1'** (7 mg, 1 mol%), trimethylacetaldehyde (86 mg, 1 mmol) and acetonitrile (2.5 mL) was heated at 50 °C for 6 h with a O₂ balloon (1 atm. O₂). After reaction, the mixture was filtered to remove the solid phase and the filtrate was analyzed with GC-MS.

Cyclic Carbonation Reaction. The synthesis of cyclic carbonates was carried out in a glass tube with magnetic bar. A mixture of epoxides (2 mmol), **2** (0.3 mol%, 10 mg), and *n*-butylammonium bromide (*n*Bu₄NBr) (2.5 mol%, 16 mg) was heated at 50°C for 4 h with a CO₂ balloon (1 atm. CO₂). After reaction, the mixture was filtered to remove the solid phase and the filtrate was analyzed with GC-MS.

Recycle Experiments

The recyclability of **1'** and **2** was tested with five consecutive runs. After reaction, the solid phase was filtered and collected. By washing

with DMF and MeOH for three times, the catalyst **1**' was dried under 200 °C for 5 h under vacuum pressure, the catalyst **2** was dried under 80 °C for 4 h. Then they were used for another run.

Acknowledgements

We are grateful to the National Key Research and Development Program of China (2016YFA0602900) and the National Natural Science Foundation of China (Nos. 21372087 and 21420102003) for the financial support.

Keywords: Metal-organic frameworks • crystal structure • Cyanosilylation • Olefin Epoxidation • CO₂ fixation

- [1] (a) H. Furukawa and O. M. Yaghi, *J. Am. Chem. Soc.*, 2009, **131**, 8875; (b) E. Barea, C. Montoro and J. A. Navarro, *Chem. Soc. Rev.*, 2014, **43**, 5419; (c) P. Kumar, K.-H. Kim, E. E. Kwon and J. E. Szulejko, *J. Mater. Chem. A*, 2016, **4**, 345.
- [2] (a) Z. Hu, B. J. Deibert and J. Li, *Chem. Soc. Rev.*, 2014, **43**, 5815; (b) J. Rocha, L. D. Carlos, F. A. Paz and D. Ananias, *Chem. Soc. Rev.*, 2011, **40**, 926; (c) J. Heine and K. Müller-Buschbaum, *Chem. Soc. Rev.*, 2013, **42**, 9232; (d) M. D. Allendorf, C. A. Bauer, R. K. Bhakta and R. J. T. Houk, *Chem. Soc. Rev.*, 2009, **38**, 1330; (e) Y. Cui, Y. Yue, G. Qian and B. Chen, *Chem. Rev.*, 2012, **112**, 1126.
- [3] (a) M. Kurmoo, *Chem. Soc. Rev.*, 2009, **38**, 1353; (b) S. Behrens and I. Appel, *Curr. Opin. Biotech.*, 2016, **39**, 89; (c) K. Liu, X. Zhang, X. Meng, W. Shi, P. Cheng and A. K. Powell, *Chem. Soc. Rev.*, 2016, **45**, 2423.
- [4] (a) B. L. Chen, S. C. Xiang, and G. D. Qian, *Acc. Chem. Res.*, 2010, **43**, 1115; (b) L. E. Kreno, K. Leong, O. K. Farha, M. Allendorf, R. P. Van Duyne and J. T. Hupp, *Chem. Rev.*, 2012, **112**, 1105.
- [5] (a) J. W. Liu, L. F. Chen, H. Cui, J. Y. Zhang, L. Zhang and C. Y. Su, *Chem. Soc. Rev.*, 2014, **43**, 6011; (b) L. Q. Ma, C. Abney and W. B. Lin, *Chem. Soc. Rev.*, 2009, **38**, 1248; (c) Y. Liu, W. Xuan and Y. Cui, *Adv. Mater.*, 2010, **22**, 4112; (d) M. Zhao, S. Ou and C. D. Wu, *Acc. Chem. Res.*, 2014, **47**, 1199; (f) K. K. Tanabe and S. M. Cohen, *Chem. Soc. Rev.*, 2011, **40**, 498; (g) D. B. Shi, Y. W. Ren, H. F. Jiang, B. W. Cai and J. X. Lu, *Inorg. Chem.*, 2012, **51**, 6498; (h) D. B. Shi, Y. W. Ren, H. F. Jiang, J. X. Lu and X. F. Cheng, *Dalton Trans.*, 2013, **42**, 484.
- [6] (a) N. L. Rosi, J. Eckert, M. Eddaoudi, D. T. Vodak, J. Kim, M. O'Keeffe and O. M. Yaghi, *Science*, 2003, **300**, 1127; (b) S. S. Kaye, A. Dailly, O. M. Yaghi and J. R. Long, *J. Am. Chem. Soc.*, 2007, **129**, 14176; (c) H. L. Li, M. Eddaoudi, T. L. Groy, and O. M. Yaghi, *J. Am. Chem. Soc.*, 1998, **120**, 8571.
- [7] (a) H. Furukawa, N. Ko, Y. B. Go, N. Aratani, S. B. Choi, E. Choi, A. Ö. Yazaydin, R. Q. Snurr, M. O'Keeffe, J. Kim and O. M. Yaghi, *Science*, 2010, **329**, 424; (b) A. Lan, K. Li, H. Wu, D. H. Olson, T. J. Emge, W. Ki, M. Hong and J. Li, *Angew. Chem. Int. Ed.*, 2009, **48**, 2334; (c) C. L. Hobday, R. J. Marshall, C. F. Murphie, J. Sotelo, T. Richards, D. R. Allan, T. Duren, F. X. Coudert, R. S. Forgan, C. A. Morrison, S. A. Moggach and T. D. Bennett, *Angew. Chem. Int. Ed.*, 2016, **55**, 2401; (d) J. An and N. L. Rosi, *J. Am. Chem. Soc.*, 2010, **132**, 5578; (e) C. Wang, Z. Xie, K. E. deKrafft and W. Lin, *J. Am. Chem. Soc.*, 2011, **133**, 13445; (f) A. Bhunia, S. Dey, J. M. Moreno, U. Diaz, P. Concepcion, K. V. Hecke, C. Janiak and P. V. Voort, *Chem. Commun.*, 2016, **52**, 1401; (g) Q. R. Fang, G. S. Zhu, Z. Jin, Y. Y. Ji, J. W. Ye, M. Xue, H. Yang, Y. Wang and S. L. Qiu, *Angew. Chem. Int. Ed.*, 2007, **46**, 6638; (h) B. Fernández, G. Beobide, I. Sánchez, F. Carrasco-Marín, J. M. Seco, A. J. Calahorra, J. Cepeda and A. Rodríguez-Diéguez, *CrystEngComm.*, 2016, **18**, 1282; (i) V. T. Nguyen, H. Q. Ngo, D. T. Le, T. Truong and N. T. S. Phan, *Chem. Eng. J.*, 2016, **284**, 778.
- [8] (a) A. Schaate, P. Roy, A. Godt, J. Lippke, F. Waltz, M. Wiebcke and P. Behrens, *Chem. Eur. J.*, 2011, **17**, 6643; (b) M. Carboni, C. W. Abney, S. Liu and W. Lin, *Chem. Sci.*, 2013, **4**, 2396; (c) C. A. Williams, A. J. Blake, C. Wilson, P. Hubberstey and M. Schröder, *Cryst. Growth. Des.*, 2008, **8**, 911.
- [9] (a) H. X. Deng, S. Grunder, K. E. Cordova, C. Valente, H. Furukawa, M. Hmadeh, F. Gandara, A. C. Whalley, Z. Liu, S. Asahina, H. Kazumori, M. O'Keeffe, O. Terasaki, J. F. Stoddart and O. M. Yaghi, *Science*, 2012, **336**, 1018; (b) H. Furukawa, F. Gandara, Y. B. Zhang, J. C. Jiang, W. L. Queen, M. R. Hudson and O. M. Yaghi, *J. Am. Chem. Soc.*, 2014, **136**, 4369; (c) D. X. Xue, A. J. Cairns, Y. Belmabkhout, L. Wojtas, Y. L. Liu, M. H. Alkordi and M. Eddaoudi, *J. Am. Chem. Soc.*, 2013, **135**, 7660; (d) P. Horcajada, F. Salles, S. Wuttke, T. Devic, D. Heurax, G. Maurin, A. Vimont, M. Daturi, O. David, E. Magnier, N. Stock, Y. Filinchuk, D. Popov, C. Riekel, G. Férey and C. Serre, *J. Am. Chem. Soc.*, 2011, **133**, 17839; (e) S. Q. Qdgaard, B. Bouchevreau, K. Hylland, L. P. Wu, R. Blom, C. Grande, U. Olsbye, M. Tilset and K. P. Lillerud, *Inorg. Chem.*, 2016, **55**, 1986; (f) Y. Kim, J. H. Song, W. R. Lee, W. J. Phang, K. S. Lim and C. S. Hong, *Cryst. Growth. Des.*, 2014, **14**, 1933; (g) X. Z. Wang, D. R. Zhu, Y. Xu, J. Yang, X. Shen, J. Zhou, N. Fei, X. K. Ke and L. M. Peng, *Cryst. Growth. Des.*, 2010, **10**, 887; (h) T. Gao, X. Z. Wang, H. X. Gu, Y. Xu, X. Shen and D. R. Zhu, *CrystEngComm.*, 2012, **14**, 5905; (i) S. Nagata, H. Sato, K. Sugikawa, K. Kokadoa and K. Sada, *CrystEngComm.*, 2012, **14**, 4137; (j) S. Yuan, Y. P. Chen, J. S. Qin, W. G. Lu, X. Wang, Q. Zhang, M. Bosch, T. F. Liu, X. Z. Lian and H. C. Zhou, *Angew. Chem. Int. Ed.*, 2015, **54**, 14696; (k) H. Furukawa, J. Kim, N. W. Ockwig, M. O'Keeffe and O. M. Yaghi, *J. Am. Chem. Soc.*, 2008, **130**, 11650; (l) R. Babarao, C. J. Coghlan, D. Rankine, W. M. Bloch, G. K. Gransbury, H. Sato, S. Kitagawa, C. J. Sumby, M. R. Hill and C. J. Doonan, *Chem. Commun.*, 2014, **50**, 3238; (m) A. D. Burrows, C. G. Frost, M. F. Mahon and C. Richardson, *Chem. Commun.*, 2009, 4218; (n) L. Z. Chen, Q. J. Pan, X. X. Cao and F. M. Wang, *CrystEngComm.*, 2016, **18**, 1944; (o) P. V. Dau and S. M. Cohen, *Inorg. Chem.*, 2015, **54**, 3134; (p) A. Ferguson, L. Liu, S. J. Tapperwijn, D. Perl, F. X. Coudert, S. V. Cleuvenbergen, T. Verbiest, M. A. van der Veen and S. G. Telfer, *Nat. Chem.*, 2016, **8**, 250; (q) L. L. Gong, X. F. Feng, F. Luó, X. F. Yi and A. M. Zheng, *Green. Chem.*, 2016, **18**, 2047; (r) T. Ishiwata, Y. Furukawa, K. Sugikawa, K. Kokado and K. Sada, *J. Am. Chem. Soc.*, 2013, **135**, 5427; (s) T. D. Keene, D. Rankine, J. D. Evans, P. D. Southon, C. J. Kepert, J. B. Aitken, C. J. Sumby and C. J. Doonan, *Dalton. Trans.*, 2013, **42**, 7871; (t) Y. L. Li, D. Zhao, Y. Zhao, P. Wang, H. W. Wang and W. Y. Sun, *Dalton. Trans.*, 2016, **45**, 8816; (u) D. Rankine, A. Avellaneda, M. R. Hill, C. J. Doonan and C. J. Sumby, *Chem. Commun.*, 2012, **48**, 10328; (v) D. Rankine, T. D. Keene, C. J. Doonan and C. J. Sumby, *Cryst. Growth. Des.*, 2014, **14**, 5710; (w) A. Santra and P. K. Bharadwaj, *Cryst. Growth. Des.*, 2014, **14**, 1476; (x) T. Song, J. Yu, Y. Cui, Y. Yang and G. Qian, *Dalton. Trans.*, 2016, **45**, 4218; (y) X. Wang, J. Zhao, Y. Zhao, H. Xu, X. Shen, D. R. Zhu and S. Jing, *Dalton. Trans.*, 2015, **44**, 9281; (z) N. Zhang, J. Y. Zhang, Q. X. Jia, W. Deng and E. Q. Gao, *RSC Adv.*, 2015, **5**, 70772.
- [10] (a) I. Boldog, L. Xing, A. Schulz and C. Janiak, *C. R. Chimie*, 2012, **15**, 866; (b) R. K. Das, A. Aijaz, M. K. Sharma, P. Lama and P. K. Bharadwaj, *Chem. Eur. J.*, 2012, **18**, 6866; (c) M. Lee, S. M. Shin, N. Jeong and P. K. Thallapally, *Dalton. Trans.*, 2015, **44**, 9349; (d) T. K. Pal, R. Katoch, A. Garg and P. K. Bharadwaj, *Cryst. Growth. Des.*, 2015, **15**, 4526; (e) T. H. Park, K. Koh, A. G. Wong-Foy and A. J. Matzger, *Cryst. Growth. Des.*, 2011, **11**, 2059; (f) R. Singh and P. K. Bharadwaj, *Cryst. Growth. Des.*, 2013, **13**, 3722; (g) R. F. Wu and T. L. Zhang, *Z. Anorg. Allg. Chem.*, 2012, **638**, 282; (h) R. F. Wu, Y. J. Zhu and W. Jin, *Z. Anorg. Allg. Chem.*, 2013, **639**, 2290.
- [11] (a) G. L. Wen, F. W. Wang, D. F. Liu, X. L. Wang, M. Gu and Y. Y. Wang, *Inorg. Chim. Acta.*, 2016, **447**, 6; (b) M. Kobalz, J. Lincke, K. Kobalz, O. Erhart, J. Bergmann, D. Lassig, M. Lange, J. Mollmer, R. Glaser, R. Staudt and H. Krautscheid, *Inorg. Chem.*, 2016, **55**, 3030.
- [12] (a) M. Eddaoudi, J. Kim, M. O'Keeffe and O. M. Yaghi, *J. Am. Chem. Soc.*, 2002, **124**, 376; (b) K. S. Jeong, Y. B. Go, S. M. Shin, S. J. Lee, J. Kim, O. M. Yaghi and N. Jeong, *Chem. Sci.*, 2011, **2**, 877.
- [13] M. Eddaoudi, J. Kim, N. Rosi, D. Vodak, J. Wachter, M. O'Keeffe and O. M. Yaghi, *Science*, 2002, **295**, 469.
- [14] (a) S. Ma, X. S. Wang, C. D. Collier, E. S. Manis and H. C. Zhou, *Inorg. Chem.*, 2007, **46**, 8499; (b) A. D. Burrows, C. G. Frost, M. F. Mahon and C. Richardson, *Angew. Chem. Int. Ed.*, 2008, **47**, 8482; (c) A. P. Nelson, O. K. Farha, K. L. Mulfort and J. T. Hupp, *J. Am. Chem. Soc.*, 2009, **131**, 458; (d) A.

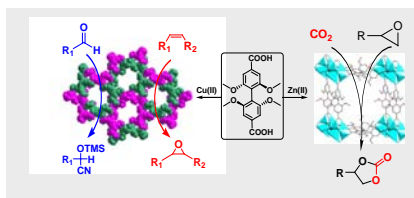
- D. Burrows, L. C. Fisher, D. Hodgson, M. F. Mahon, N. F. Cessford, T. Düren, C. Richardson and S. P. Rigby, *CrystEngComm.*, 2012, **14**, 188; (e) W. W. Lestari, P. Lonneck, M. B. Sarosi, H. C. Streit, M. Adlung, C. Wickleder, M. Handke, W. D. Einicke, R. Glaser and E. Hey-Hawkins, *CrystEngComm.*, 2013, **15**, 3874; (f) P. Shen, W. W. He, D. Y. Du, H. L. Jiang, S. L. Li, Z. L. Lang, Z. M. Su, Q. Fu and Y. Q. Lan, *Chem. Sci.*, 2014, **5**, 1368; (g) T. Moradpour, A. Abbasi and K. Van Hecke, *J. Solid. State. Chem.*, 2015, **228**, 36.
- [15] (a) H. Y. Ren, R. X. Yao and X. M. Zhang, *Inorg. Chem.*, 2015, **54**, 6312; (b) X. Cui, M. C. Xu, L. J. Zhang, R. X. Yao and X. M. Zhang, *Dalton Trans.*, 2015, **44**, 12711; (c) J. Yang, X. Q. Wang, F. N. Dai, L. L. Zhang, R. M. Wang, and D. F. Sun, *Inorg. Chem.*, 2014, **53**, 10649; (d) M. Oh, L. Rajput, D. Kim, D. Moon and M. S. Lah, *Inorg. Chem.*, 2013, **52**, 3891; (e) Y. Q. Lan, H. L. Jiang, S. L. Li and Q. Xu, *Inorg. Chem.*, 2012, **51**, 7484; (f) Q. X. Yao, J. L. Sun, K. Li, J. Su, M. V. Peskov and X. D. Zou, *Dalton trans.*, 2012, **41**, 3953.
- [16] C. K. Brozek, V. K. Michaelis, T. C. Ong, L. Bellarosa, N. López, R. G. Griffin and M. Dincă, *ACS Cent. Sci.*, 2015, **1**, 252.
- [17] (a) H. M. He, F. X. Sun, S. Q. Ma and G. S. Zhu, *Inorg. Chem.*, 2016, **55**, 9071; (b) Y. Hijikata, S. Sakaki, *Inorg. Chem.*, 2014, **53**, 2417; (c) L. J. Li, J. Bell, S. F. Tang, X. X. Lv, C. Wang, Y. L. Xing, X. B. Zhao and K. M. Thomas, *Chem. Mater.*, 2014, **26**, 4679.
- [18] (a) Q. Q. Dang, Y. F. Zhan, L. N. Duan and X. M. Zhang, *Dalton Trans.*, 2015, **44**, 20027; (b) L. J. Zhang, C. Y. Han, Q. Q. Dang, Y. H. Wang and X. M. Zhang, *RSC Adv.*, 2015, **5**, 24293. (c) X. Wang, L. Zhang, J. Yang, F. Dai, R. Wang and D. Sun, *Chem. Asian. J.*, 2015, **10**, 1535.
- [19] Y. Zhu, Y. M. Wang, S. Y. Zhao, P. Liu, C. Wei, Y. L. Wu, C. K. Xia and J. M. Xie, *Inorg. Chem.*, 2014, **53**, 7692.
- [20] (a) X. L. Yang and C. D. Wu, *Inorg. Chem.*, 2014, **53**, 4797; (b) Z. Zhang, L. Zhang, L. Wojtas, P. Nugent, M. Eddaoudi and M. J. Zaworotko, *J. Am. Chem. Soc.*, 2012, **134**, 924.
- [21] (a) S. Parshamoni, J. Telangae, S. Sanda and S. Konar, *Chem. Asian. J.*, 2016, **11**, 540; (b) P. Cancino, V. Paredes-García, P. Aguirre and E. Spodine, *Catal. Sci. Technol.*, 2014, **4**, 2599; (c) S. Abednatanzi, A. Abbasi and M. Masteri-Farahani, *New J. Chem.*, 2015, **39**, 5322; (d) Y. Qi, Y. Luan, J. Yu, X. Peng and G. Wang, *Chem. Eur. J.*, 2015, **21**, 1589.
- [22] K. Zhang, O. K. Farha, J. T. Hupp and S. T. Nguyen, *Acs. Catal.*, 2015, **5**, 4859.
- [23] (a) J. L. Song, Z. F. Zhang, S. Q. Hu, T. B. Wu, T. Jiang and B. X. Han, *Green. Chem.*, 2009, **11**, 1031; (b) W. Kleist, F. Jutz, M. Maciejewski and A. Baiker, *Eur. J. Inorg. Chem.*, 2009, 3552; (c) H. Y. Choa, D. A. Yanga, J. Kima, S. Y. Jeongb and W. S. Ahn, *Catal. Today.*, 2012, **185**, 35; (d) D. A. Yang, H. Y. Cho, J. Kim, S. T. Yang and W. S. Ahn, *Energy. Environ. Sci.*, 2012, **5**, 6465; (e) C. M. Miralda, E. E. Macias, M. Zhu, P. Ratnasamy and M. A. Carreon, *ACS. Catal.*, 2012, **2**, 180; (f) X. Zhou, Y. Zhang, X. G. Yang, L. Z. Zhao and G. Y. Wang, *J. Mol. Catal. A: Chem.*, 2012, **361**, 12. (g) Y. W. Ren, X. F. Cheng, S. R. Yang, C. R. Qi, H. F. Jiang and Q. P. Mao, *Dalton. Trans.*, 2013, **42**, 9930; (h) Y. W. Ren, Y. C. Shi, J. X. Chen, S. R. Yang, C. R. Qi and H. F. Jiang, *RSC Adv.*, 2013, **3**, 2167; (i) J. Kim, S. N. Kim, H. G. Jang, G. Seo and W. S. Ahn, *Appl. Catal. A-Gen.*, 2013, **453**, 175; (j) W. J. Gao, Y. Chen, Y. H. Niu, K. Williams, L. Cash, P. J. Perez, L. Wojtas, J. F. Cai, Y. S. Chen and S. Q. Ma, *Angew. Chem. Int. Ed.*, 2014, **53**, 2615; (k) M. H. Beyzavi, R. C. Klet, S. Tussupbayev, J. Borycz, N. A. Vermeulen, C. J. Cramer, J. F. Stoddart, J. T. Hupp and O. K. Farha, *J. Am. Chem. Soc.*, 2014, **136**, 15861; (l) Z. Zhou, C. He, J. H. Xiu, L. Yang and C. Y. Duan, *J. Am. Chem. Soc.*, 2015, **137**, 15066; (m) A. C. Kathalikkattil, R. Roshan, J. Tharun, R. Babu, G. S. Jeong, D. W. Kim, S. J. Cho and D. W. Park, *Chem. Commun.*, 2016, **52**, 280; (n) R. Babu, A. C. Kathalikkattil, R. Roshan, J. Tharun, D. W. Kim and D. W. Park, *Green. Chem.*, 2016, **18**, 232. (o) Q. X. Han, B. Qi, W. M. Ren, C. He, J. Y. Niu and C. Y. Duan, *Nat. Commun.*, 2015, **6**:10007 doi: 10.1038/ncomms10007.
- [24] J. Sun, S. I. Fujita, F. Zhao and M. Arai, *Appl. Catal. A-Gen.*, 2005, **287**, 221.
- [25] A. W. Kleij, *Dalton Trans.*, 2009, 4635.
- [26] (a) M. H. Anthofer, M. E. Wilhelm, M. Cokoja, M. Drees, W. A. Herrmann and F. E. Kühn, *ChemCatChem*, 2015, **7**, 94; (b) Y. W. Ren, O. Jiang, H. Zeng, Q. P. Mao and H. F. Jiang, *RSC Adv.*, 2016, **6**, 3243; (c) Y. W. Ren, J. G. Chen, C. R. Qi, and H. F. Jiang, *ChemCatChem*, 2015, **7**, 1535.
- [27] G. M. Sheldrick, *Acta. Crystallogr. A.*, 2008, **64**, 112.
- [28] A. L. Spek, *PLATON, A Multipurpose Crystallographic Tool*, Utrecht University, The Netherlands, 2002.

Entry for the Table of Contents (Please choose one layout)

Layout 1:

FULL PAPER

Three-dimensional Cu-MOF based on 2,2',6,6'-tetramethoxy-4,4'-biphenyldicarboxylic acid exhibits high activities for cyanosilylation reaction and olefin epoxidation reaction. Zn-MOF based on the same ligand displays an excellent catalytic activity for the synthesis of cyclic carbonates from epoxides and CO₂ under mild conditions.



MOFs catalysis

Jiawei Li, Yanwei Ren, Chaorong Qi and Huanfeng Jiang****Page No. – Page No.****Full *Meta*-substituted 4,4'-Biphenyldicarboxylate Based MOFs: Synthesis, Structures and Catalytic activities**